

# AN EXPERIMENTAL STUDY OF THE INDENTATION BEHAVIOUR OF Al FOAM

X. Wang\* – X. Peng – Z. Guo

State Key Laboratory of Coal Mine Disaster Dynamics and Control, Department of Engineering Mechanics, Postdoctoral Station of Mechanics, Chongqing University, Chongqing 400040, China

## ARTICLE INFO

### Article history:

Received: 31.01.2013.

Received in revised form: 08.02.2013.

Accepted: 08.02.2013.

### Keywords:

Al foam

Indentation

Tear energy

Energy absorbing

## Abstract:

*The indentation response of a closed-cell Al foam under the flat-end cylindrical indenter was experimentally investigated. The effects of indenter sizes, relative density of Al foam and boundary condition on the mechanical and energy absorption characteristics of indentation were also investigated. Experimental results show that the indentation load-displacement response obtained using the flat-end cylindrical indenter is similar to that observed under uniaxial compression. Cross-sectional views of the indented specimens show that the deformation is confined only to the region directly under the indenter with very little lateral spread, and that the indentation deformation of Al foam is non-uniform. The tear energy and energy absorbing efficiency of Al foam is not related with the indenter diameter and relative density of Al foam. By increasing the indenter diameter or decreasing relative density, the indentation hardness is linearly decreased, but the energy absorbing capability linearly increases with an increase in indenter diameter or an increase in relative density. At a certain indentation depth range, the difference between rigid foundation and the indentation response of Al foam under simply supported conditions can be ignored.*

## 1 Introduction

Metal foam is a new class of materials with low densities and novel physical, mechanical, thermal, electrical and acoustic properties. Therefore, it has the potential for use in lightweight structural components and in energy absorption and has received extensive attention [1-2].

The low impact (or indentation) behavior of metal foam has been widely investigated in the recent years. Many of these works are experimental studies on the behavior of metal foam. Olurin and Wang et

al. [3,4] have investigated the indentation response of metallic foams for different indenter geometry, indenter sizes, and the foam density. They have extracted tear energy for material by using a simple analysis and found it to be in agreement with similar failure bearing data, and with the mode I steady state fracture energy. Andrews et al. [5] have investigated the size-dependence of the plastic strength of metallic foams and found that the indentation stress varies with the indenter diameter, showing a size effect. Dynamic indentation and penetration tests by Ramachandra et al. [6] and Li et

\* Corresponding author. Tel.: +86 15334520880; fax: +86 2365102421  
E-mail address: wxz@cqu.edu.cn.

al. [7] showed that the indentation resistance was increased significantly at velocities greater than 10 m/s.

Kwon and Wojcik [8] used a finite element model of a sandwich composite to investigate stresses, strains, deflections and failure modes during impact. Methods of predicting the deformation and fracture behaviour of sandwich panels with foam cores when subjected to quasi-static indentation have been worked out by Tania [9] and Xie [10]. Sudheer et al. [11] experimentally investigated the deep indentation response of a closed-cell Al foam under different rates of penetration. Numerical simulations and experimental investigations of quasi-static indentation into polymeric foams have been studied by several authors, e.g. [12,13].

The main purpose of this research is to (experimentally) characterize the indentation resistance of metal foam panels under the flat-end cylindrical indenter (by the experimental method). The effects of indenter sizes, relative density of Al foam and boundary condition on the mechanical and energy absorption characteristics of indentation were also investigated.

## 2 Experimental

Available closed-cell Al foam is used in this study. This foam is processed by the direct foaming technique that uses  $TiH_2$  powders as an additive to the molten metal for foaming. The foam has an average cell size of  $\sim 2$  mm and cell wall thickness of the foam ranged from 80 to 100  $\mu m$ . Typical macroscopic view of the foam is shown in Fig. 1. As seen from the figure, the cell sizes for this particular metal foam are locally very inhomogeneous, but conversely have an overall uniform morphology.

Indentation tests were performed on three foams with different relative densities: 9, 20 and 29%. An electromechanical testing machine (INSTRAN-5569) was used with a flat-end circular cylindrical indenter ( $D=12.7, 16, 20, 25.4$ mm in diameter) in displacement control at a speed of 1mm/min and the load and the load-line displacement are recorded. The maximum indentation depth was about 8mm. The specimens are supported by a rigid foundation, so the overall bending is limited. Five samples were tested for each type of specimen. To minimize the effects of friction, the indenters were lubricated with PTFE spray.

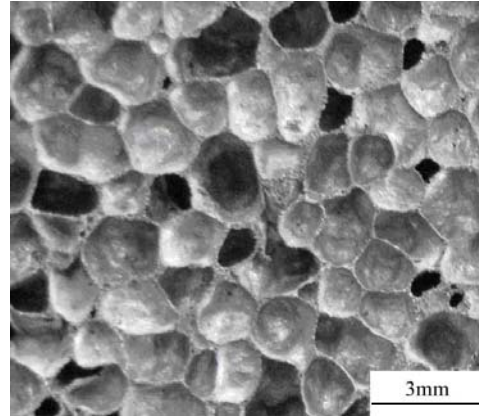


Figure 1. A macroscopic view of the closed-cell Al foam, used in the current study.

Reproducible hardness data require that the indenters have a diameter,  $D$ , that is large compared with the cell size,  $d$  ( $D/d > 7$ ). Edge effects are avoided if the indentations are at least one indenter diameter away from the edges of the plate. The dimensions of rectangular samples were  $100 \times 100 \times 15$ mm<sup>3</sup>. Fig. 2 shows a schematic model of the indentation test setup.

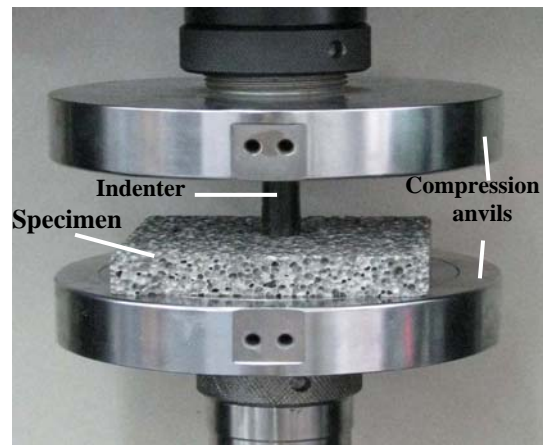


Figure 2. Indentation test setup of Al foam.

## 3 Results analysis and discussion

### 3.1 Indentation response characters

The total force on the indenter is the sum of energy/force necessary to crush the foam beneath the indenter and to tear it at the edges of the indenter [14], that is

$$P = P_{crushing} + P_{tearing} = S\sigma_{pl}^* + 2\pi a\gamma \quad (1)$$

Where  $P$  is the total load,  $a$  is the radius of indenter and  $S$  is the contact area between indenter and foam,  $\sigma_{pl}^*$  is the compressive plateau stress of the foam and  $\gamma$  is its tear energy.

Typical load-displacement curves for indentation of Al foam with different relative densities under different diameters indenter are shown in Fig. 3 and Fig. 4. Due to the elastic-plastic behavior of Al foam, the load-indentation curves have a generally non-linear shape. The load-displacement indentation response of Al foam is similar to that in uniaxial compression (see [10]). At the beginning of the testing, when the indentation magnitude is low, the load-indentation response is linear. This behavior continues until the moment when an initiation of plastic deformation (crushing of the metal foam) is triggered. After that, load approaches a plateau value, prior to an increase in stress when there is an interaction with the back face of the plate. The oscillations in the load-displacement response are due to repeating cycles of yield, collapse and densification (see Fig. 3). However, a couple of differences between uniaxial compression and indentation  $P-h$  data are noteworthy. For example, the difference pertains to the nature of the plastic response. Whereas the  $P-h$  curve in uniaxial compression appears to be independent of  $h$  within the plastic collapse regime, the force required for penetrating the indenter gradually but definitely increases with  $h$ . Two factors contribute to this response. As the deformation proceeds, an increasingly larger crushed zone beneath the indenter will offer resistance to its further penetration, which results in a steeper load-displacement curve, in comparison with a monotonic compression load-displacement curve. Second, by increasing  $h$ , the tearing resistance at the indenter perimeter is increased contributing to a gradual rise in  $P$ .

Overall, by increasing indenter diameters, the contact load is increased. This can be understood from the fact that by increasing the diameter of indenter, the contact area will be increased correspondingly at the same indentation depth. The contact load also increases with an increase in relative density. This is determined by the properties of the material, such as the elastic modulus, yield strength and shear modulus of Al foam, which are strongly dependent on the relative density of Al foam<sup>[1]</sup>.

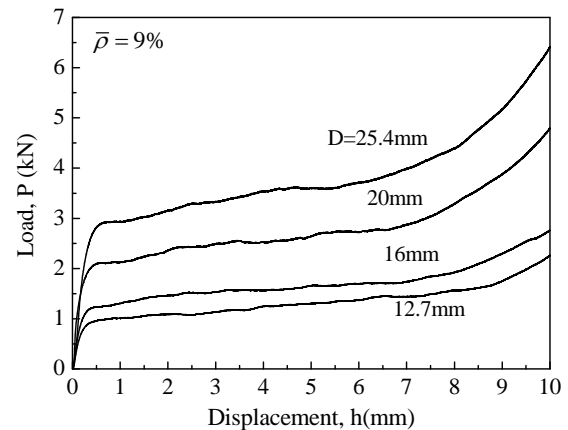


Figure 3.  $P-h$  curves of Al foam under different diameters of the flat-end cylindrical indenters.

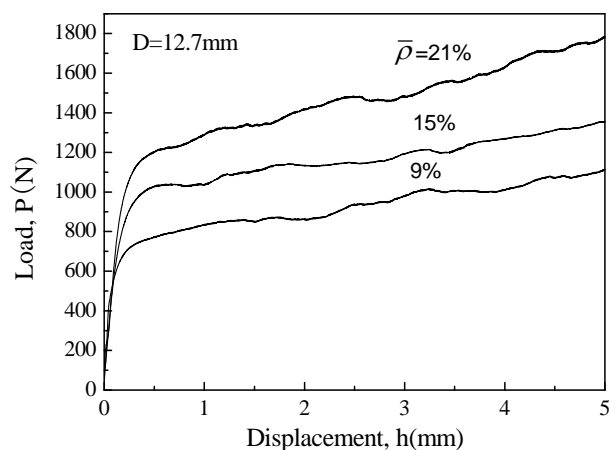


Figure 4.  $P-h$  curves of Al foam with different relative densities under the flat-end cylindrical indenters.

The above mentioned specimens of indentation test are supported by a rigid foundation. In addition, the indentation response of Al foam under simply supported boundary conditions is studied. Metal blocks are placed at the bottom edge of the specimens to mimic the simply supported boundary conditions. The experiment results are shown in Fig. 5 and Fig. 6.

We can see from Fig. 5, the boundary conditions exert little effect on the curve segments of indentation response curves before the load drop. Different boundary conditions exert an influence on the deformation of Al foam if Al foam is subjected to overall bending.

When the indentation depth reaches a critical value, the indentation load based on rigid boundary conditions has a rapid and sudden increase, due to the foam cells under the indenter densification. The role of rigid foundation of Al foam is significant at this time. The indentation response curve of the Al foam under simple boundary conditions has also an obvious turning point and the indentation load has a rapid sudden drop. This is because the back of Al foam corresponding to indenter is free of traction. The part of deformation of Al foam contributed to the overall bending when the indentation depth reaches a critical value. At a certain indentation depth range, the difference between rigid foundation and simply supported boundary conditions on the indentation response of Al foam can be ignored. We can clearly see that at the back region of Al foam under simple boundary conditions pile-up and fracture under the indenter occurred, as shown in Fig. 6.

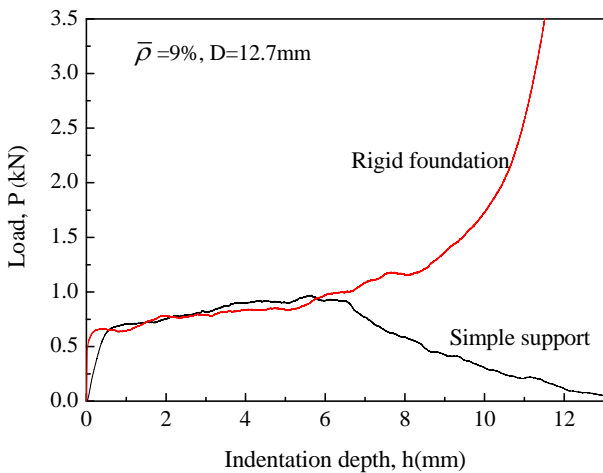


Figure 5. Typical  $P-h$  curves of Al foam for different boundary conditions under the FEP indentation.

### 3.2 Deformation mechanism

In order to study microscopic deformation mechanism of Al foam, the indentation deformation zone of Al foam is cut along the longitudinal axis of the direction by electric discharge method, morphology of indentation deformation zone is photographed by Olympus SZX12 microscope as shown in Fig. 7.

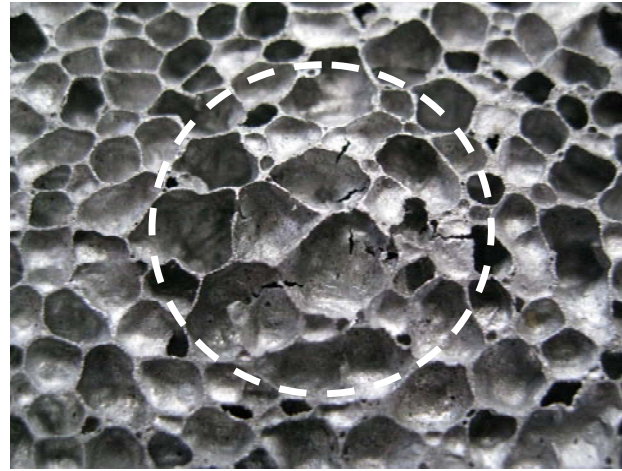


Figure 6. Macrographs of Al foam back region for simple boundary condition under the FEP indentation with depth of 6mm.

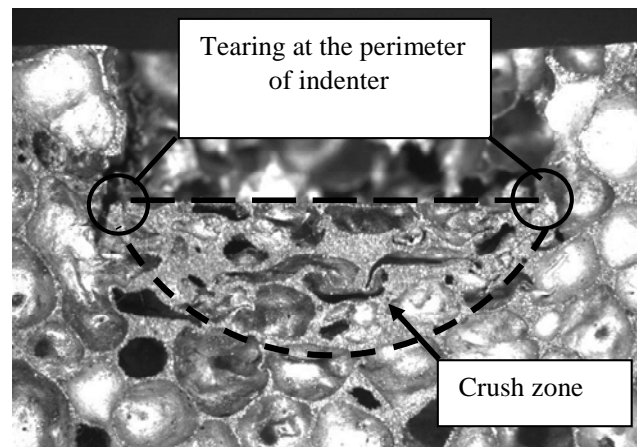


Figure 7. Cross-sectional morphology of Al foam after indentation.

The plastic deformation of Al foam was localized in the region just underneath the indenter and has very little lateral spreading in Fig. 7, because metallic foams are plastically compressible with a plastic Poisson's ratio near zero<sup>[11-13]</sup>. The deformation is extensive within the zone of plasticity wherein cells have been crushed and whereas outside it, the material is in pristine condition. However, the deformation during indentation is not entirely confined to the region of the compacted zone beneath the indenter; buckling of cells located somewhat farther away can occur.

Furthermore, Fig. 7 reveals that the shape of the deformation zone is identical with that of numerical simulation<sup>[15]</sup> and is approximately a spherical cap. Visual observations of the surface of the cylindrical cavity created by the indenter indicate clean tearing

with no indication of bending or shear deformation of the cells.

In order to evaluate the effectiveness of FE model in ref.15, the experimental result is compared to the result of FE simulation in a certain zone of indentation (Fig. 8).

As shown in Fig. 8, the FE simulation result agrees well with the experimental result, which shows that the FE model can be used to predict the indentation response of Al foam.

### 3.3 Mechanical properties and energy absorption characteristics

Mechanical properties and energy absorption characteristics of metallic foams can be investigated through an indentation test. Indentation tests have been used for more than a century now to measure the properties of engineering materials. The most commonly used indentation testing technique is the hardness test. An important advantage of this technique lies in the fact that it requires a relatively small volume of material, thus enabling several repeating experiments on relatively smaller specimens.

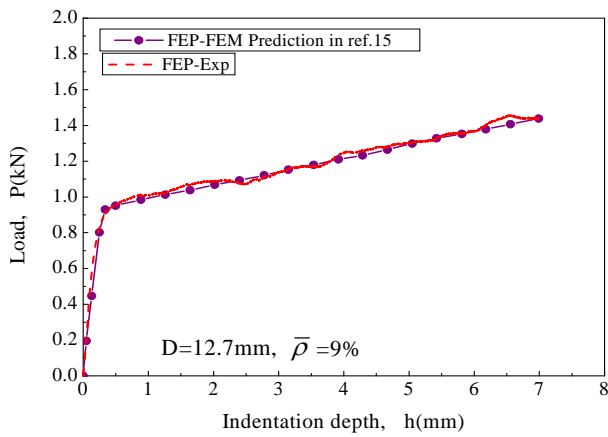


Figure 8. Experimental versus FE simulation curves of Al foam.

Mechanical properties obtained from the indentation test are the hardness ( $H$ ), tear energy ( $\gamma$ ) and shear strength ( $\tau^*$ ).  $H$  defined as:

$$H = \frac{P}{A} \quad (2)$$

Where  $P$  is the applied load and  $A$  is the projected contact area of indentation. For flat-end cylindrical

indenter, the projected contact area is  $A = \pi a^2$ . Rearranging Equation 1 gives

$$\gamma = \frac{P - S\sigma_{pl}^*}{2\pi a} = \frac{P - \pi a^2 \sigma_{pl}^*}{2\pi a} = \frac{(\bar{p} - \sigma_{pl}^*)a}{2} \quad (3)$$

Where  $\bar{p}$  is the total indentation pressure. The relationship of tear energy and shear strength is as follows:

$$\tau^* = \frac{\gamma}{d} \quad (4)$$

Where  $d$  is the diameter of foam cell.

Energy absorbing capability,  $w$ , and energy absorbing efficiency,  $\eta$ , are two important parameters to evaluate energy absorption characteristics of Al foam.  $W$ , the absorbed energy per unit volume in a certain strain interval  $[\varepsilon_1, \varepsilon_2]$  is equal to the area below the stress-strain curve and can be expressed as

$$w = \int_{\varepsilon_1}^{\varepsilon_2} \sigma(\varepsilon) d\varepsilon \quad (5)$$

$\eta$  is defined as the ratio of energy absorbed by an ideal energy absorber to that absorbed by the actual foam:

$$\eta = \frac{\int_{\varepsilon_1}^{\varepsilon_2} \sigma(\varepsilon) d\varepsilon}{\sigma_0(\varepsilon_2 - \varepsilon_1)} \quad (6)$$

$H$ ,  $\gamma$ ,  $w$  and  $\eta$  are calculated according to  $P-h$  response curves of Al foam with different indenter sizes and relative densities at the same indentation depth,  $h_c = 6mm$ , as shown in Fig. 9 – Fig. 12.

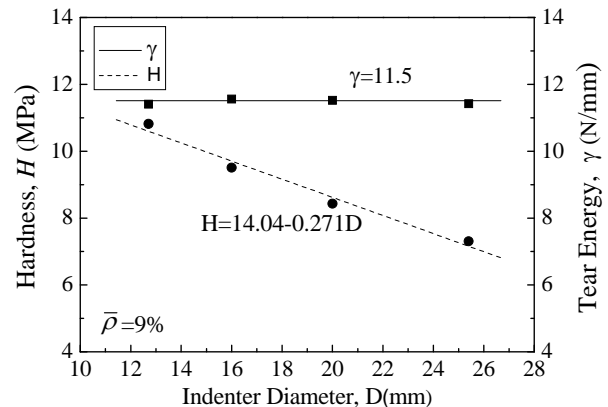


Figure 9.  $H - D$  and  $\gamma - D$  curves of Al foam.

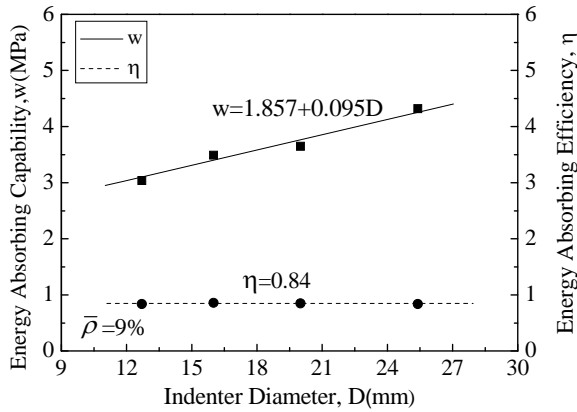


Figure 10.  $w - D$  and  $\eta - D$  curves of Al foam.

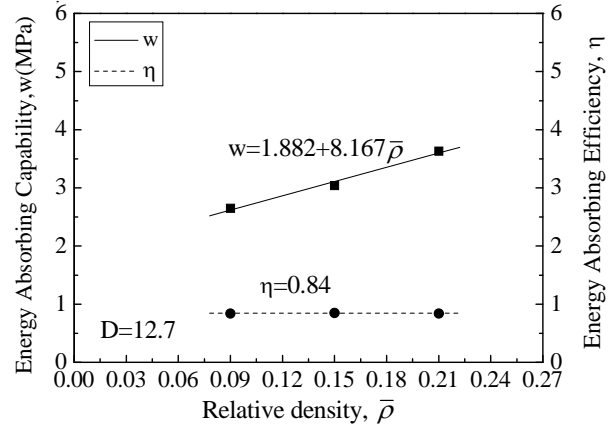


Figure 12.  $w - \bar{\rho}$  and  $\eta - \bar{\rho}$  curves of Al foam.

We can see from Fig. 9-12, the indentation hardness linearly decreases by increasing indenter size and linearly increases by increasing relative density. Energy absorbing capability of Al foam linearly increases with the increase in indenter sizes or relative density. The tear energy and energy absorbing efficiency are independent of indenter sizes and relative density of Al foam, and the average values are 11.5 and 0.84.

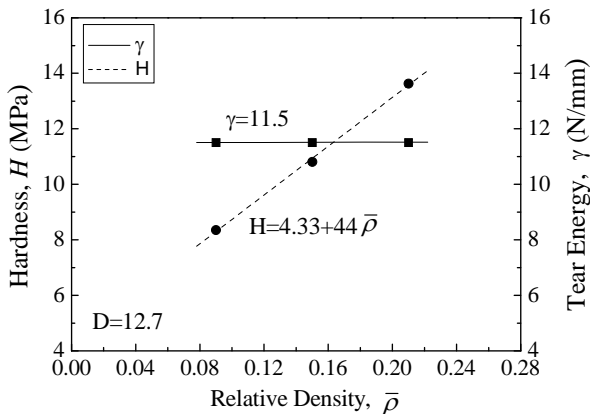


Figure 11.  $H - \bar{\rho}$  and  $\gamma - \bar{\rho}$  curves of Al foam.

#### 4 Conclusions

The main aim of this current study is to investigate the indentation behavior of Al foam by experiments under the flat-end cylindrical indenter. Comprehensive indentation tests were conducted to elaborate the effect of indenter sizes and relative density on the indentation hardness, energy absorbing capability and energy absorbing efficiency of Al foam. The key results of this investigation can be summarized as follows:

- (1) The indentation response curve of Al foam under the flat-end cylindrical indenter is similar to that in uniaxial compression, but there have been some differences, such as deformation mechanism.
- (2) The experiment results show that the compacted zone is restricted to the region directly under the indenter and has very little lateral spreading, but tearing of foam cells occur in the vicinity of the densified region. Furthermore, the experiment and simulation correctly reveal that the shape of the deformation zone is similar to that of porous rock and is hemispherical.
- (3) Mechanical properties can be obtained from the indentation test, such as tear energy ( $\gamma$ ) and shear strength ( $\tau^*$ ). It was found that by increasing the indenter size, the indentation hardness is linearly decreased and by increasing relative density, it is linearly increased. Energy absorbing capability of Al foam is linearly increased when the indenter sizes or relative density are increased. The tear energy and energy absorbing efficiency are independent of indenter sizes and relative density of Al foam.
- (4) At a certain indentation depth range, the

difference between rigid foundation and indentation responses of Al foam under simply supported boundary conditions can be ignored.

### Acknowledgments

This work are performed with the financial support by the Key Project of Chinese Ministry of Education (No. 313059), the Fundamental Research Funds for the Central Universities (Project No. CDJRC10240002,CDJZR10240014,CDJZR12240067,CDJZR1224071,CDJZR12248801,CDJZR12110072), China Postdoctoral Science Foundation (No. 2011M500067) and NSFC (No. 11272362) .

### References

- [1] Ashby, M.F., Evans, A.G., Fleck, N.A., Gibson, L.J., Hutchinson, J.W., Wadley, H.N.G.: *Metal Foams: A Design Guide*. Butterworth-Heinemann, UK, 2000.
- [2] Gibson, L.J., Ashby, M.F.: *Cellular Solids: Structure and Properties*, 2nd edition. Cambridge University Press, UK, 1997.
- [3] Olurin, O.B., Fleck, F.A., Ashby, M.F. *Indentation resistance of an aluminum foam*, Scripta Materialia, 43(2000), 983-989.
- [4] Wang, X., Wu, L., Wang, S.: *Mechanical response of a closed-cell Al foam under static indentation*, Acta Materialia Compositae Sinica, 27 (2010), 77-83.
- [5] Andrews E.W., Gioux, G., Onck P., Gibson, L.J.: *Size effects in ductile cellular solids. Part II: experimental result*, Int J Mechanical Sciences. 43(2001), 701-708.
- [6] Ramachandra, S., Sudheer, P., Ramamurty, U.: *Impact energy absorption in an Al foam at low velocities*. Scripta Materialia, 49 (2003), 741-752.
- [7] Q, M., Li, R.N.: *Maharaj and S. R. Reid. Penetration Resistance of Aluminium Foam*, Int J Vehicle Design, 37(2005), 175-184.
- [8] Kwon, Y.W., Wojcik, G.W.: *Impact study of sandwich composite structures with delamination*, J. Compos Mater, 32 (1998), 406-413.
- [9] Vodenitcharova, T., Kabir, K., Hoffman M.: *Indentation of metallic foam core sandwich panels with soft aluminium face sheets*, Materials Science & Engineering A, 558(2012), 175-185.
- [10] Xie Z., Zheng Z., Yu J.: *Localized indentation of sandwich panels with metallic foam core*, Analytical models for two types of indenters, Composites: Part B, 31 (2013), 212-217.
- [11] Sudheer, Kumar P., Ramachandra, S., and Ramamurty, U.: *Effect of displacement-rate on the indentation behavior of an aluminum foam*, Materials Science and Engineering A, 347 (2003), 330-337.
- [12] Flores-Johnson, E.A., Li Q.M.: *Indentation into polymeric foams*, International Journal of Solids and Structures, 47 (2010), pp. 1987-1995.
- [13] Briody, C., Duignan, B., Jerrams, S., Tiernan, J.: *The implementation of a visco-hyperelastic numerical material model for simulating the behaviour of polymer foam materials*, Computational Materials Science. 4 (2012), 231-245.
- [14] Ramamurty, U., Kumaran, M.C.: *Mechanical property extraction through conical indentation of a closed-cell aluminum foam*, Acta Materialia, 52 (2004), 181-189.
- [15] Wang, X., Zhou, G.: *The Indentation Behavior of Closed-cell Al Foam under the Flat-end Cylindrical Indenter*, Materials Science Forum, 704-705(2012), 960-966.

